

SCIENTIFIC REPORTS



OPEN

Characterisation of a stable laboratory co-culture of acidophilic nanoorganisms

Susanne Krause¹, Andreas Bremges^{3,4}, Philipp C. Münch^{3,5}, Alice C. McHardy³ & Johannes Gescher^{1,2}

This study describes the laboratory cultivation of ARMAN (Archaeal Richmond Mine Acidophilic Nanoorganisms). After 2.5 years of successive transfers in an anoxic medium containing ferric sulfate as an electron acceptor, a consortium was attained that is comprised of two members of the order *Thermoplasmatales*, a member of a proposed ARMAN group, as well as a fungus. The 16S rRNA identity of one archaeon is only 91.6% compared to the most closely related isolate *Thermogymnomonas acidicola*. Hence, this organism is the first member of a new genus. The enrichment culture is dominated by this microorganism and the ARMAN. The third archaeon in the community seems to be present in minor quantities and has a 100% 16S rRNA identity to the recently isolated *Cuniculiplasma divulgatum*. The enriched ARMAN species is most probably incapable of sugar metabolism because the key genes for sugar catabolism and anabolism could not be identified in the metagenome. Metatranscriptomic analysis suggests that the TCA cycle funneled with amino acids is the main metabolic pathway used by the archaea of the community. Microscopic analysis revealed that growth of the ARMAN is supported by the formation of cell aggregates. These might enable feeding of the ARMAN by or on other community members.

The question of the smallest autonomous living cell is an intensely discussed topic in microbiology. In 1999, the Steering Group for the Workshop on Size Limits of Very Small Microorganisms defined the lower theoretical limit for an autonomous living cell inhabiting all necessary components to 0.008–0.014 μm^3 ¹. Early findings of ultra-small microorganisms, e.g. “ultramicrobacteria” in sea-water² and “dwarf cells” or “nanobacteria” in soils^{3,4}, and the question of the potential medical relevance⁵ of some of these cells were the starting point and motivation for a new research direction. Nevertheless, some of these nanobacteria were questioned later for being microcrystalline apatite⁶ or microbial starvation forms⁷. Still, there are several organisms with cell sizes close to or even below the mentioned theoretical limit that were identified in different habitats in the last century.

Filtration of water samples with 0.2 or 0.1 μm filters and subsequent sequencing of the 16S rRNA genes of the organisms has revealed that the enriched small or ultra-small microbes belong to candidate divisions that are widespread in nature but lack any cultured representative^{8,9}. Luef *et al.*⁹ even hypothesized that it might be a general characteristic of previously uncultivable bacterial phyla that the organisms belonging to these phyla are small⁹. Thus far, isolated ultramicrobacteria belong to different phyla including *Actinobacteria*¹⁰, *Bacteroidetes*¹¹ or *Alphaproteobacteria*^{12,13}. They have cell volumes between $<0.1 \mu\text{m}^3$ and $<0.004 \mu\text{m}^3$, and their energy metabolism is described as chemoorganotrophic, heterotrophic or facultatively parasitic. Nevertheless, detailed information about optimal growth conditions, ecological role and corresponding genomic or transcriptomic data are often not available.

Nanoarchaeum equitans and the recently cultured “*Nanopusillus acidilobi*” are the only ultra-small archaea that have been cultivated and characterized under laboratory conditions so far. The genome of *N. equitans* is only ~0.5 Mbp in size. It lacks nearly all genes essential for primary biosynthesis as well as the central and energy metabolism¹⁴, which indicates a strong dependency on its host *Ignicoccus hospitalis*. Interestingly, *I. hospitalis*

¹Department of Applied Biology, Karlsruhe Institute of Technology (KIT), Karlsruhe, Germany. ²Institute for Biological Interfaces, Karlsruhe Institute of Technology (KIT), Eggenstein-Leopoldshafen, Germany. ³Computational Biology of Infection Research, Helmholtz Centre for Infection Research, Braunschweig, Germany. ⁴German Center for Infection Research (DZIF), partner site Hannover-Braunschweig, Braunschweig, Germany. ⁵Max von Pettenkofer-Institute of Hygiene and Medical Microbiology, Ludwig-Maximilians-University of Munich, Munich, Germany. Correspondence and requests for materials should be addressed to J.G. (email: johannes.gescher@kit.edu)

cells do not divide if more than two *N. equitans* cells infect them. Still, generation time and final cell densities of *I. hospitalis* are not affected by infection¹⁵. Despite the absence of detectable damage or genomic regulatory changes to its host, *N. equitans* is described as a nutritional parasite¹⁶. Like *N. equitans*, “*Nanopusillus acidilobi*” is an obligate ecto-symbiont or parasite with a reduced genome (~0.6 kbp). It lacks the majority of the necessary genetic information for energy metabolism and primary biosynthetic pathways except for several genes encoding proteins that are putatively involved in glycolysis and gluconeogenesis¹⁷.

The genomes of members of the not yet isolated Archaeal Richmond Mine Acidophilic Nanoorganisms (ARMAN) are ~0.5 Mbp larger than the genomes of *N. equitans* and “*N. acidilobi*”. They contain the necessary information for key functions of a central carbon metabolism¹⁸. This is indicative of a more independent lifestyle. The ARMAN were first detected by Baker *et al.* in 2006¹⁹. Since then, five different ARMAN groups (ARMAN-1 to ARMAN-5) were found in acidophilic biofilms that thrive at the Richmond Mine localized at the Iron Mountains in California¹⁸. ARMAN-1 and -2 belong to the phylum *Micrarchaeota*, while groups -4 and -5 are part of the *Parvarchaeota*. The phylogenetic position of ARMAN-3 is not known, since a 16S rRNA gene sequence is not available so far. The organisms are ellipsoid cells with volumes of 0.009 μm^3 to 0.04 μm^3 and are surrounded by a cell wall. The average number of ribosomes that were detected per cell was only 92. Furthermore, most cells have enigmatic tubular structures of unknown function²⁰. Genomic and proteomic data assembled from metagenomes of ARMAN-2, -4 and -5 revealed that the organisms have a complete or nearly complete tricarboxylic acid cycle, but that only ARMAN-4 and -5 have further genes for glycolytic pathways, the pentose phosphate pathway, and glycerol utilization¹⁸.

Still, the overall metabolism of the organisms, as well as the question of a putative dependency on other community members remain unclear. Moreover, prediction of the physiological capabilities of the ARMAN is highly complex if not even momentarily impossible since 25–38% of the predicted genes do not match sequences in public databases. Nevertheless, ARMAN are prominent members of submerged acid mine drainage (AMD) biofilms especially in anoxic parts²¹, which indicates a prominent role within these biocoenoses.

The 16S rRNA genes of ARMAN were also found in other ecosystems affected by AMD^{22,23}. One of these is the former pyrite mine “Drei Kronen und Ehrt” in the Harz Mountains in Germany. Here, the microorganisms are embedded in gel-like biofilms, which resemble stalactite-formations²⁴. These biofilms grow at average pH values of 2.0 to 2.5 and are characterized by an outer oxic rim and an inner anoxic core. The rim of the biofilm is mostly composed of chemolithoautotrophic bacteria that thrive using ferrous iron as energy and electron source and oxygen as electron acceptor. The anoxic center contains several different acidophilic archaea including ARMAN²⁵.

This study describes the enrichment of ARMAN from biofilms of the “Drei Kronen und Ehrt” mine and the physiological, metagenomic and metatranscriptomic analysis of the enrichment culture. With long-term selective culturing experiments, it was possible to obtain very low diversity enrichment cultures of ARMAN. These are dominated by a not-yet cultured member of the *Thermoplasmatales* and an ARMAN-1 related organism. Analyses of the enrichment cultures as well as metagenomic and metatranscriptomic data offer new insights into the lifestyle of the previously uncultured ARMAN as well as two novel members of the *Thermoplasmatales*.

Results and Discussion

Enrichment process. In 2013, Ziegler *et al.* described stalactite like biofilms that grow on the ceiling of an abundant pyrite mine in the Harz mountains in Germany²⁵. Organisms belonging to the ARMAN as well as members of the *Thermoplasmatales* were detected within the anoxic core of the biofilms. The goal of this study was to produce a pure or at least highly enriched ARMAN culture to understand potential ecological dependencies of the organisms. Hence, the enrichment process used an anoxic medium containing casein and yeast extract as surrogates for biomass formed by chemolithoautotrophic primary producers of the biofilms. Furthermore, ferric sulfate was added as potential electron acceptor because iron and sulfate were prominent members of the water dripping from the biofilms²⁴. Finally, the headspace of the hungate tubes was flushed with a hydrogen/carbon dioxide mixture (80%/20%) because there was also evidence for potential methanogenic activity in the biofilm, which could be supported by the release of hydrogen from fermentative microorganisms. A mixture of four antibiotics was added to select for archaeal growth. After 1.5 years, bacteria could no longer be observed using CARD-FISH or PCR-analysis. Hence, the addition of antibiotics was omitted from this point onward.

After 2.5 years, the cultures showed a rather stable behavior and could be transferred every 10 weeks. Ferric iron reduction could be observed using the ferrozine assay within the individual growth intervals of the cultures. Moreover, addition of ferric sulfate was necessary for archaeal growth. Therefore, dissimilatory iron reduction seems to be an important trait of at least one member of the archaeal community. At this point, CARD-FISH analysis revealed the presence of archaea, ARMAN and a fungus (Supplementary Figure S1). Of note, the archaea probe does not hybridize to ARMAN species, which indicates the presence of at least one other archaeal species in the enrichment.

Metagenome and phylogenetic analysis. We could reconstruct the genomes of three different archaea. Hence the CARD-FISH analysis using archaea probes displayed the presence of two different organisms. Supplementary Figure S2 shows the taxonomic profiles for metagenomes determined with Taxator-tk²⁶. These profiles corroborate the CARD-FISH results and reveal that the majority of the available sequence (~80%) can be assigned to the archaea, while the remaining part cannot be assigned to a taxonomic group. Unfortunately, we could not find clear evidence for DNA or RNA that could be assigned to the fungus in the enrichment cultures, possibly because the fungus was underrepresented at the point of sampling and due to the robust cell structure, which might have hampered DNA-isolation. The sequence data suggests a community that consists predominantly of a novel member of the *Thermoplasmatales* which is most closely related to *Thermogymnomonas acidicola* (91.6% identity, 1206 bp) and *Cuniculiplasma divulgatum* (91.7% identity, 1206 bp) (Supplementary Table S1 shows an overview of most closely related sequences). Moreover, an organism belonging to the ARMAN group

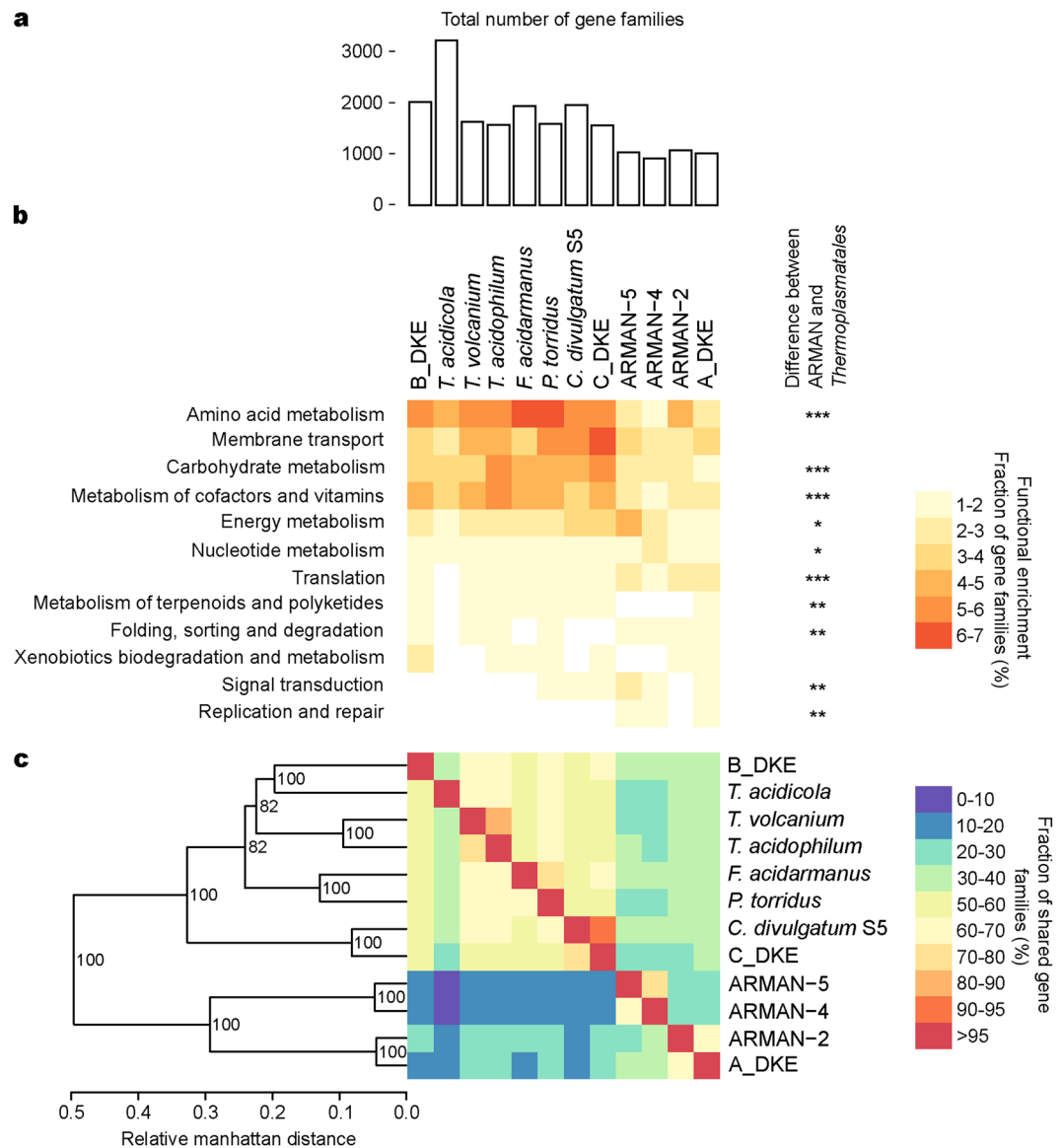


Figure 2. (a) Total number of orthoMCL families found in indicated genomes. (b) Functional enrichment analysis of orthologous genes. The heat map depicts the percentage of orthoMCL groups of each genome assigned to each indicated functional category. Stars indicate FDR corrected significance levels for difference in the number of orthoMCL families between the four ARMAN and eight *Thermoplasmatales* genomes (one star for value below '0.05', two for '0.01' and three for '0.001'). (c) Heat map and hierarchical clustering dendrogram depicting the percentage of gene families shared between genomes. Node labels in the tree indicate bootstrap support after 100 iterations. Columns are normalized based on the total number of gene families found in genomes.

on the 16S rRNA genes, A_DKE seems to be most closely related to ARMAN-2. This was also corroborated by further comparative genome analysis (Fig. 3). The GC-content of ARMAN-2 is rather similar to A_DKE, while ARMAN-4 and -5 share lower GC values. Furthermore, the number of similar genes – defined by expected E-values lower $1e-100$ – also seems to cluster A_DKE with ARMAN-2 while ARMAN-4 and ARMAN-5 build via that analysis a second group (Fig. 3a). Using an automated assignment of genes to central metabolic pathways using the KEGG database we could highlight the presence and similarity within and between the different ARMAN genomes. It seems that all organisms share a similar set of genes involved in the citric acid cycle and in respiration. In contrary, genes involved in glycolysis/gluconeogenesis, the pentose phosphate pathway, the Enter-Doudoroff pathway or the β -oxidation are not as similar and wide spread within the genomes of the organisms.

Overall, the genome of A_DKE differs from previously sequenced ARMAN species in terms of sugar metabolism. Baker *et al.*¹⁸ described a pentose phosphate pathway for ARMAN-4 and -5 and an incomplete glycolysis for ARMAN-2¹⁸. In contrast, we could not identify genes encoding the necessary enzymes for the conversion of glucose to pyruvate. Moreover, we could identify only two potential genes that could be involved in the pentose phosphate

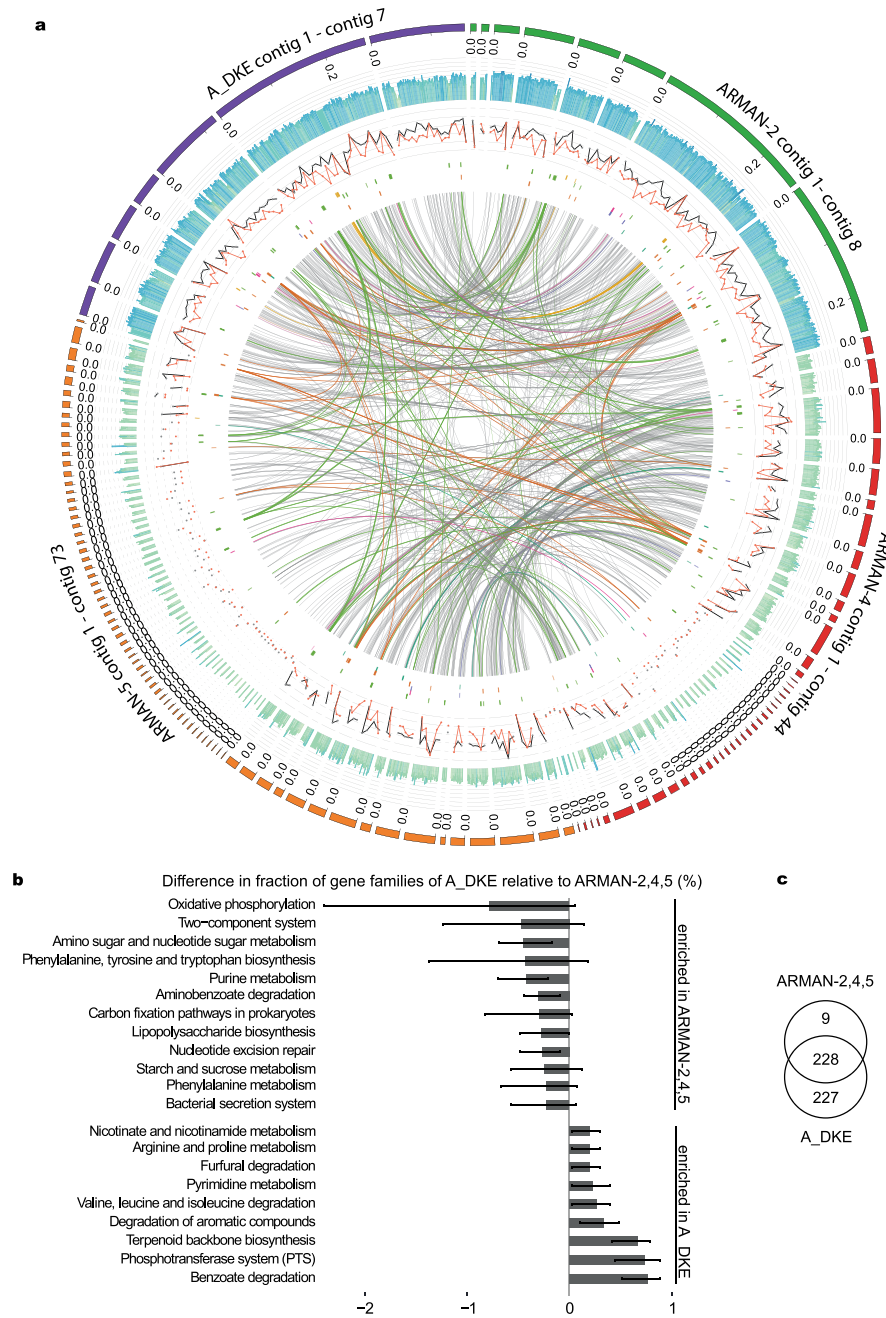


Figure 3. (a) Genome comparison of ARMAN-2/-4/-5 and A_DKE generated with Donut (unpublished). From outer track to inner track: (1) GC content (higher values colored in blue, lower values are colored green). (2) ORF density (annotated and hypothetical) within a sliding window over the genomes visualized in black. ORF density of hypothetical ORFs visualized in red based on a sliding window approach. (3–8) Matches to KEGG terms in this order: beta-Oxidation (yellow), Oxidative phosphorylation (green), Entner–Doudoroff pathway (pink), pentose phosphate pathway (purple), citric acid cycle (orange), glycolysis/gluconeogenesis (blue). Lines within the inner segment indicate significant similarity between ORFs of the individual genomes and are colored according to KEGG terms if they fully overlap these. Contig sizes are visualized in Mb. (b) Bar plot showing the over-abundance of functions based on *de novo* inferred gene families based on orthoMCL analysis of three ARMAN genomes and the A_DKE genome. The length of the bars corresponds to the mean difference in the fraction of gene families annotated with the indicated functional group. Lines show the difference to the ARMAN genomes with the minimal and the maximal fraction. Only functional groups are shown that differ in more than 0.2% or less than -0.2% . (c) Venn diagram of gene families shared between indicated genomes. Gene families related to pathogenicity factors were not included in this overview.

pathway. Moreover, the genes encoding for key reactions of the ED pathway were not detectable (Supplementary Table S6). Hence, there seems to be a necessity for the uptake of hexose and pentose sugars from the environment. Furthermore, a β -oxidation of fatty acids seems to be not possible, since the genome contains only genes for a 3-hydroxyacyl-CoA dehydrogenase and an acetyl-CoA thiolase. In contrary, we detected genes for a complete tricarboxylic acid cycle (TCA), with the exception that bioinformatic analysis revealed so far only one subunit of the succinyl-CoA synthetase in A_DKE. Archaeal electron transport complexes can have unusual compositions²⁹. Nevertheless, bioinformatic analysis predicts so far only the existence of a NADH-dehydrogenase, a respiratory succinate-dehydrogenase and an ATP-synthase in the ARMAN genome. Hence, it is not clear how the energy metabolism of the organism might function. While the citric acid cycle would be a way to produce ATP/GTP, it also leads to the production of reducing-equivalents. How these reducing equivalents are transported to an electron acceptor and what this electron acceptor might be is not clear so far. Our data suggest an anoxic life style. Evidence for fermentative pathways was not found. Hence, we must assume that the organism can use either ferric iron and/or sulfate as electron acceptor (the only electron acceptors present in the medium) or that it can conduct an inter-species electron transfer to one of the other community members. Therefore, we must also assume that ARMAN species might have evolved novel components for respiratory electron transfer that are currently not detectable by bioinformatics analyses and will necessitate biochemical analysis for characterisation.

B_ and C_DKE. A dendrogram based upon the hierarchical clustering of gene families shared between genomes of five related members of the *Thermoplasmatales* (Fig. 2c) reveals that B_DKE and C_DKE cluster together with *T. acidicola*. The core genomes of the selected *Thermoplasmatales* seem to consist of 624 gene families while the overall average number of detected gene families was 1,935 + –557. A search for unique gene families (Fig. 4c, Supplementary Table S7) in B_DKE compared to C_DKE revealed 914 gene families. Most of these were annotated as ABC transporters, two-component systems or as involved in the oxidative phosphorylation (more abundant in B_DKE) (Fig. 4b). Comparative genome analysis corroborates the identity of the 16S rRNA genes of *C. divulgatum* and C_DKE. This similarity can also be observed on the genome level since most of the genes of *C. divulgatum* have a similar counterpart in C_DKE (Fig. 4a). In contrary, the genome of B_DKE contains several areas with a rather low number of similar genes compared to C_DKE, *C. divulgatum* and *T. acidicola*. As expected, the genomes of the 4 members of the *Thermoplasmatales* have overall a low percentage of genes with hypothetical function compared to the ARMAN genomes (Fig. 3a).

Both B_ and C_DKE contain all necessary enzymes for pentose formation via the non-oxidative pentose phosphate pathway similar to other members of *Thermoplasmatales*³⁰ (Supplementary Table S6). Furthermore, the genome of B_DKE contains nearly all enzymes for the branched ED pathway including the key enzyme bifunctional KDG-/KDPG-aldolase. Nevertheless, we could not find a corresponding gene to a KDG-kinase. The genome of C_DKE shows all enzymes of the non-phosphorylated variant of the ED except its key enzyme, the KDG-aldolase. Nevertheless, a complete non-phosphorylated ED was detected in the genome of *Gplasma*²⁸ and other members of the *Thermoplasmatales* like *Thermoplasma acidophilum*³¹ or *Picrophilus torridus*³². Hence, this potential lack of pathways for the catabolism of sugar compounds is not a general characteristic of similar organisms.

Sugar degradation catalyzed by the two *Thermoplasmatales* members via glycolysis can be excluded since both genomes lack evidence for an encoded phosphofructokinase, which corresponds well with the genomic data of *C. divulgatum*³³. Still, B_DKE and C_DKE show all enzymes for gluconeogenesis, with the exception of the fructose 1,6-bisphosphate (FBP) aldolase. Nevertheless, a corresponding gene for this enzyme is missing in most archaeal genomes including *Thermoplasma acidophilum*³⁴ and *Picrophilus torridus*³⁵. Results by Say and Fuchs (2010) revealed the presence of a bifunctional FBP aldolase-phosphatase with high FBP aldolase and FBP phosphatase activity, which guarantees an unidirectional gluconeogenesis pathway³⁶. This exists in nearly all archaeal groups and may be the putative ancestral gluconeogenic enzyme. A corresponding gene was found in the genomes of B_DKE and C_DKE, which likely allows both organisms to produce sugar compounds. The key enzyme for glycolysis, the phosphofructokinase, is missing also in the genomic data of *Gplasma*, whereas a bifunctional FBP aldolase-phosphatase is detectable²⁸.

B_ and C_DKE contain the genes for a complete tricarboxylic acid cycle (TCA). In contrast, genomic analyses of *C. divulgatum* PM4 and S5 revealed that 2-oxoglutarate dehydrogenase, fumarate reductase and fumarase might be missing³³. Nevertheless, Golyshina *et al.* point out that these enzyme functions could be functionally replaced by enzymes catalyzing closely related reactions that were predicted by bioinformatic analysis. The presence of succinate dehydrogenase/fumarate reductase and 2-oxoglutarate/2-oxoacid ferredoxin oxidoreductase could also be evidence for the presence of a reverse TCA cycle in the three enriched archaea. Still, the ATP citrate lyase—the third indicator gene for the reverse TCA—is missing in all three genomes. Similar to the DKE_A genome, C_DKE and B_DKE do not seem to possess a complete β -oxidation pathway. While a β -hydroxyacyl-CoA dehydrogenase was not detectable in C_DKE, B_DKE does not seem to have β -hydroxyacyl-CoA dehydratase and dehydrogenase genes.

Bioinformatic analysis predicts also in B_ and C_DKE the existence of a NADH-dehydrogenase, a respiratory succinate-dehydrogenase and an ATP-synthase. Furthermore, B_DKE and C_DKE contain corresponding genes for a cytochrome c-oxidase although genetic evidence for a cytochrome c protein is lacking. Both contain a Rieske FeS protein that is a characteristic component of complex III and it forms a gene cluster in B_DKE with a cytochrome b6-like protein that could have complex III function²⁹. In addition, at least B_DKE has a gene which most probably encodes a copper protein belonging to the plastocyanin/azurin family, which could functionally replace cytochrome c²⁹. We currently do not know how this electron transport core chain might be connected to ferric iron reduction, which is catalyzed at least by B_DKE within the community (see below). Furthermore, we detected in C_DKE only a potential part of complex III and no cytochrome c gene. Hence, it is unknown whether the latter might be a remnant of genomic reduction and selection towards a shorter electron transport chain involving only complex I and a cytochrome ubiquinol oxidase.

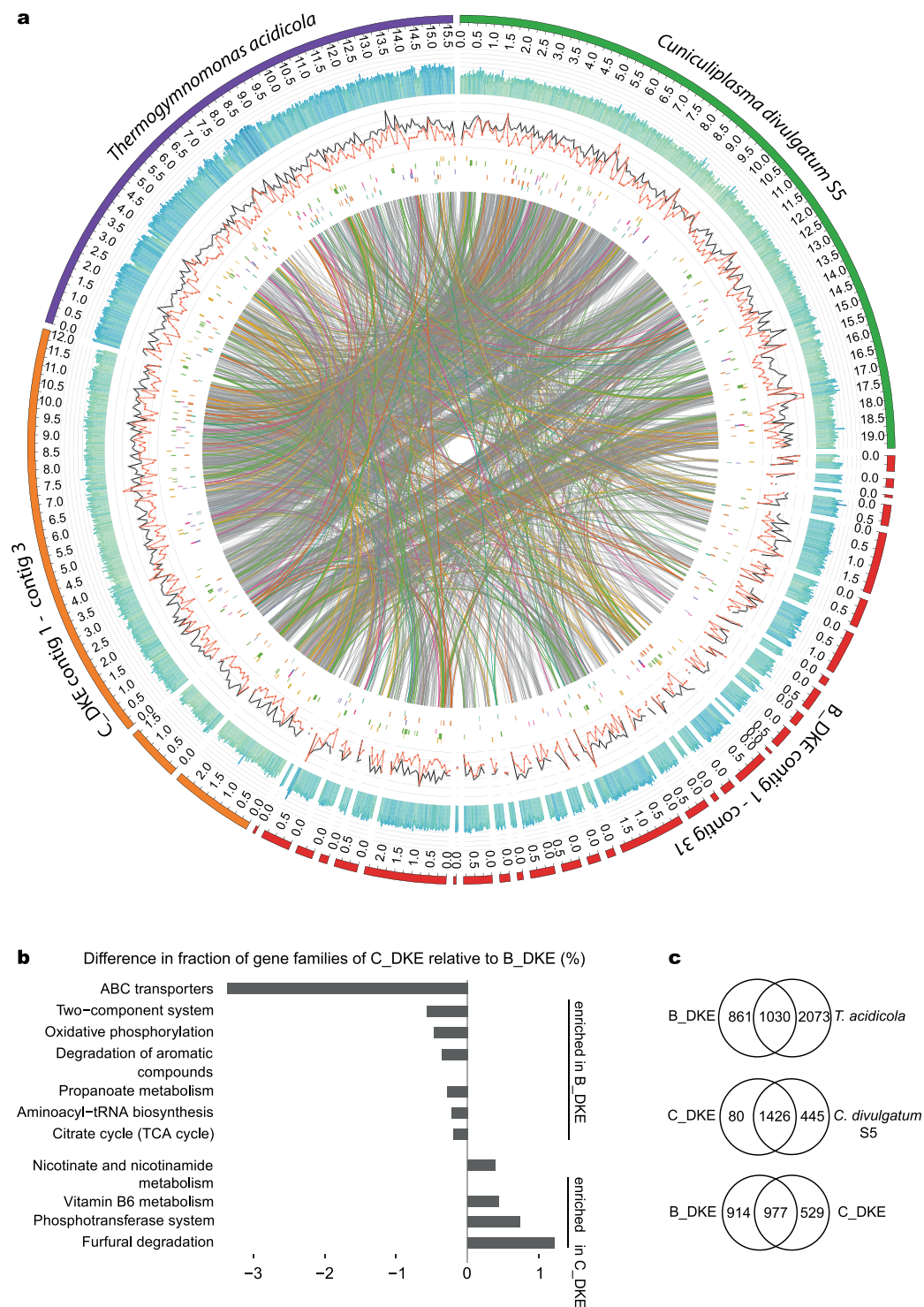


Figure 4. (a) Genome comparison of *C. divulgatum* S5, A_DKE, C_DKE and *T. acidicola* generated with Donut (unpublished). From outer track to inner track: (1) GC content (higher values colored in blue, lower values are colored green). (2) ORF density (annotated and hypothetical) within a sliding window over the genomes visualized in black. ORF density of hypothetical ORFs visualized in red based on a sliding window approach. (3–8) Matches to KEGG terms in this order beta-Oxidation (yellow), Oxidative phosphorylation (green), Entner Doudoroff pathway (pink), Pentose phosphate pathway (purple), Citric acid cycle (orange), Glycolysis/Gluconeogenesis (blue). Lines within the inner segment indicate significant similarity between ORFs between genomes and are colored according to KEGG terms if they fully overlap these. Contig sizes are visualized in Mb. (b) Bar plot showing the over-abundance of orthoMCL families assigned to indicated functional categories in C_DKE compared to B_DKE. Of these, phosphotransferase system is uniquely present in C_DKE compared to B_DKE. Only functional groups are shown that differ in more than 0.2% or less than -0.2% . (c) Venn diagram of gene families shared between indicated genomes. Gene families related to pathogenicity factors were not included in this overview.

Metatranscriptome. The ratio of sequence reads that can be referred to B_DKE, A_DKE and C_DKE is 1:0.5:0.27. Hence, all three archaea considerably contribute to the overall metatranscriptome of the study. The high content of RNA sequences that can be referred to A_DKE is surprising because all previous studies on ARMAN revealed a remarkably small number of ribosomes and because — as will be shown later — the number of ARMAN cells within the community is lower than the sum of B_DKE and C_DKE. We suggest that the considerably high content of A_DKE RNA within the metatranscriptome is evidence for active growth of the majority of ARMAN cells at sampling.

In A_DKE, 14 of the 20 most highly expressed genes encode for hypothetical proteins, which hampers the prediction of potential metabolic reactions that sustain growth of the organism. Nevertheless, the data suggests that at least glutamate could be a carbon and energy source for the organism. The glutamate dehydrogenase gene (*gdh*) is relatively high expressed (Fig. 5). The corresponding enzyme catalyzes the conversion of glutamate to 2-oxoglutarate, an intermediate of the citric acid cycle. Furthermore, transcripts could be identified for all detected genes of the citric acid cycle. Furthermore, complex I and V of the respiratory chain are expressed.

Similarly to A_DKE, the *gdh* gene is also highly expressed in B_DKE and C_DKE. In agreement with this, it can be observed in both transcriptomes that genes for TCA cycle enzymes are more highly expressed relative to the ED pathway (Fig. 5). The question about the variant of the ED remains unclear, because B_DKE expresses the 2-dehydro-3-deoxy-(phospho)gluconate (KD(P)G) aldolase as well as all enzymes for the non-phosphorylated variant of the ED and the glyceraldehyde-3-phosphate dehydrogenase (GAPN) that is involved in the semi-phosphorylated variant of the pathway and could not be detected in other members of the *Thermoplasmatales*³⁰. The C_DKE and B_DKE also express the complete set of genes necessary for gluconeogenesis and the pentose phosphate pathway. Furthermore, all detected genes encoding for electron transfer processes are highly expressed.

An analysis of the 20 most highly expressed genes (Supplementary Table S8) showed that both *Thermoplasmatales* species have high expression rates for oxidative stress proteins as well as proteins linked to electron transport process. Glutamate dehydrogenase and 2-oxoacid ferredoxin oxidoreductase are also highly expressed in C_DKE. The detected high expression rates for oxidative stress proteins could be due to the presence of trace amounts of oxygen during the cultivation, which would also indicate that oxygen could be a potential electron acceptor for the organisms. Hence, growth experiments were conducted within a glove box containing a 95% N₂/5% H₂ atmosphere. If it all, we saw slower growth of the fungus within the enrichment culture. The archaea did not seem to be affected by the strictly anoxic conditions (data not shown).

Enrichment of B_DKE and isolation of the fungus. Interestingly, omitting the addition of antibiotics lead in some cultures to an increased growth rate of B_DKE. This resulted in cultures containing only B_DKE and the fungus. The fungus was isolated from these cultures using a solidified medium described by Baker *et al.*³⁷. Fungal colonies on these plates were used for phylogenetic analysis using a primer set for ITS amplification. The phylogenetic classification of the 5.8S rRNA gene and relating ITS-DNA sequences of the fungus revealed a 99% identity to *Acidothrix acidophila*, which is an acidophilic fungus isolated from acidic soils in the Czech Republic³⁸. Of note, growth of the fungus in the medium used for the enrichment process did not lead to a reduction of the ferric sulfate. In contrary, growth of a culture containing only the fungus and B_DKE was connected to ferric sulfate reduction. Hence, B_DKE is capable of ferric iron reduction.

Timeline experiments. The dynamics and interactions within the enrichment cultures were analyzed via timeline experiments. Hence, triplicate cultures were analyzed over eleven weeks of growth. The cultures were fixed for CARD-FISH analyses twice weekly, and DNA was isolated for qPCR-based quantitative community analyses once a week. Furthermore, samples were taken for measurements of ferric iron reduction as well as control of the pH values every week. Of note, as was emphasized before, we do not have genetic information regarding the fungus so far. Therefore, we could not conclude with certainty from gene to cell quantities. Hence, the qPCR analysis was conducted only with the archaeal members of the consortium.

Analysis of the qPCR and CARD-FISH data revealed a rather similar growth behavior of A_DKE as well as B_DKE and C_DKE (Fig. 6). In the lag phase, the cell numbers increased continuously with a slightly higher amount of A_DKE cells compared to that of B_DKE and C_DKE. By week six, all organisms seemed to enter the logarithmic growth phase. From this point on, B_DKE and C_DKE began to dominate the cultures. The highest cell concentrations were reached in week eight. Thereafter, a rapid decrease in cell numbers was detected. The CARD-FISH pictures also highlight that A_DKE cells are mostly part of B_DKE or C_DKE cell agglomerates. Assuming that agglomerates are formed by extracellular polymeric material, which usually consists to a large fraction out of sugar compounds, we speculated that the biofilm growth might ensure the access to sugar for A_DKE. We emphasized in the previous section that some cultures showed faster growth during the conducted transfers and that these cultures were composed only of B_DKE and the fungus. These cultures do not show growth in the form of flocks but rather are uniform planktonic cells. Hence, the change in the growth phenotype might be the reason for decreasing A_DKE cell numbers. Supplementary Figure S3 displays the difference between the two growth phenotypes of B_DKE.

Interestingly, the ferrous iron concentrations as well as the measured pH values correlate with the growth curve data (Fig. 6). Until week six, only a slightly increased content of ferrous iron could be measured, and the pH values remained constant. From week seven on, there was a rapid ferric iron reduction along with increased growth rates. Even the pH values showed a slight decrease from this point on representing the acidification associated with the ferric iron reduction.

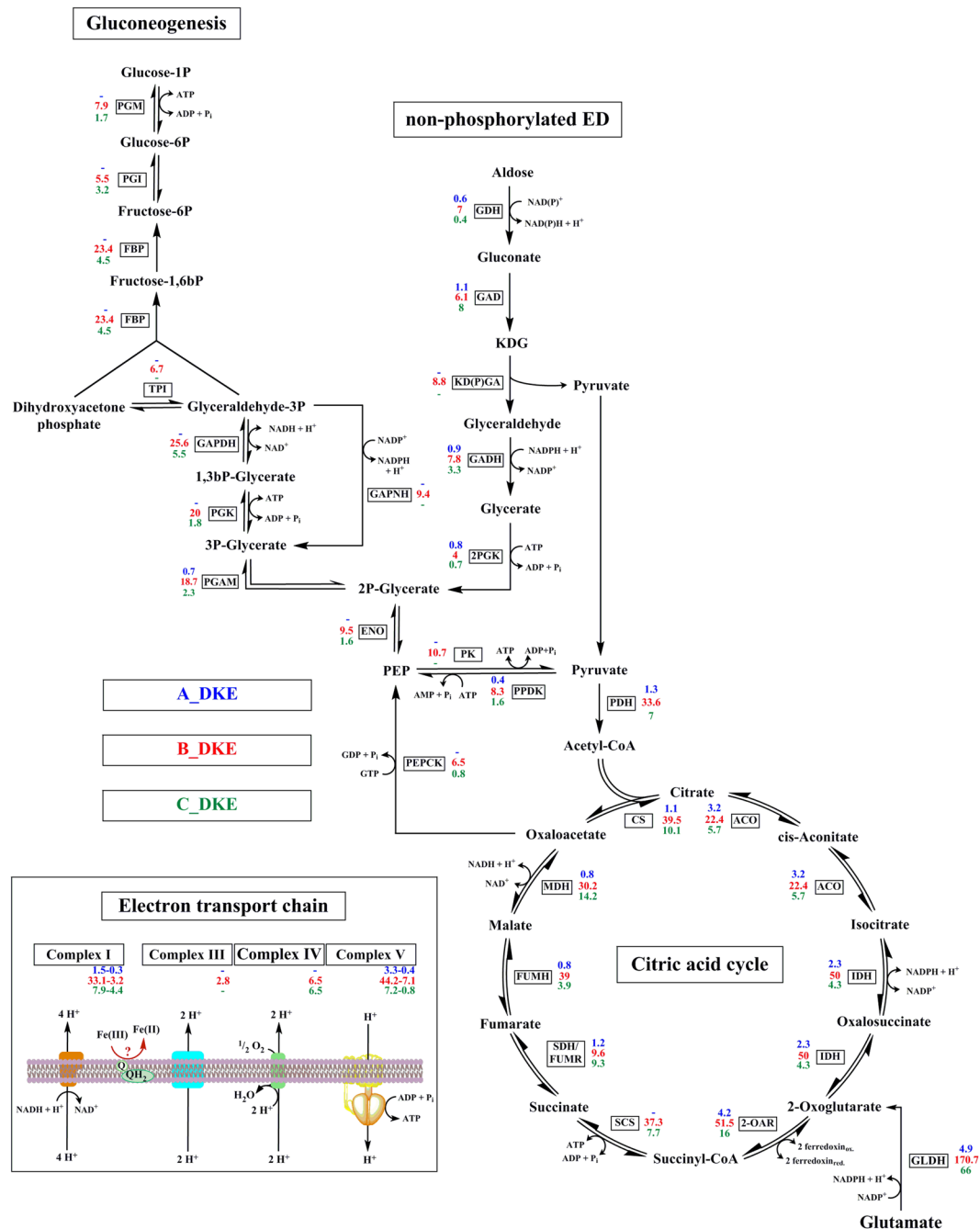


Figure 5. Postulated metabolism of all three archaea of the enrichment culture. Intermediates and catalyzing enzymes are indicated. The expression levels of the corresponding genes are listed. Blue numbers indicate RPKM-values of A_DKE, while red and green numbers refer to B_DKE and C_DKE expression, respectively. Abbreviations: PGM: phosphomannomutase/phosphoglucomutase, PGI: glucose/mannose-6-phosphate isomerase, FBP: fructose 1,6-bisphosphate aldolase/phosphatase, TPI: triosephosphate isomerase, GAPDH: glyceraldehyde-3-phosphate dehydrogenase (NAD(P)), PGK: phosphoglycerate kinase, PGAM: 2,3-bisphosphoglycerate-independent phosphoglycerate mutase, ENO: enolase, PEPCK: phosphoenolpyruvate carboxykinase (GTP), PPK: pyruvate, orthophosphate dikinase; GDH: glucose/galactose 1-dehydrogenase (NADP+), GAD: gluconate/galactonate dehydratase, KD(P)GA: 2-dehydro-3-deoxy-D-gluconate/2-dehydro-3-deoxy-phosphogluconate aldolase, GADH: D-glyceraldehyde dehydrogenase, GAPN: glyceraldehyde-3-phosphate dehydrogenase [NAD(P)+], 2PGK: glycerate 2-kinase, PK: pyruvate kinase, PDH: pyruvate dehydrogenase; CS: citrate synthase, ACO: aconitase, IDH: isocitrate dehydrogenase, SCS: succinyl-CoA synthetase, SDH/FUMR: succinate dehydrogenase/fumarate reductase, FUMH: fumarate hydratase, MDH: malate dehydrogenase.

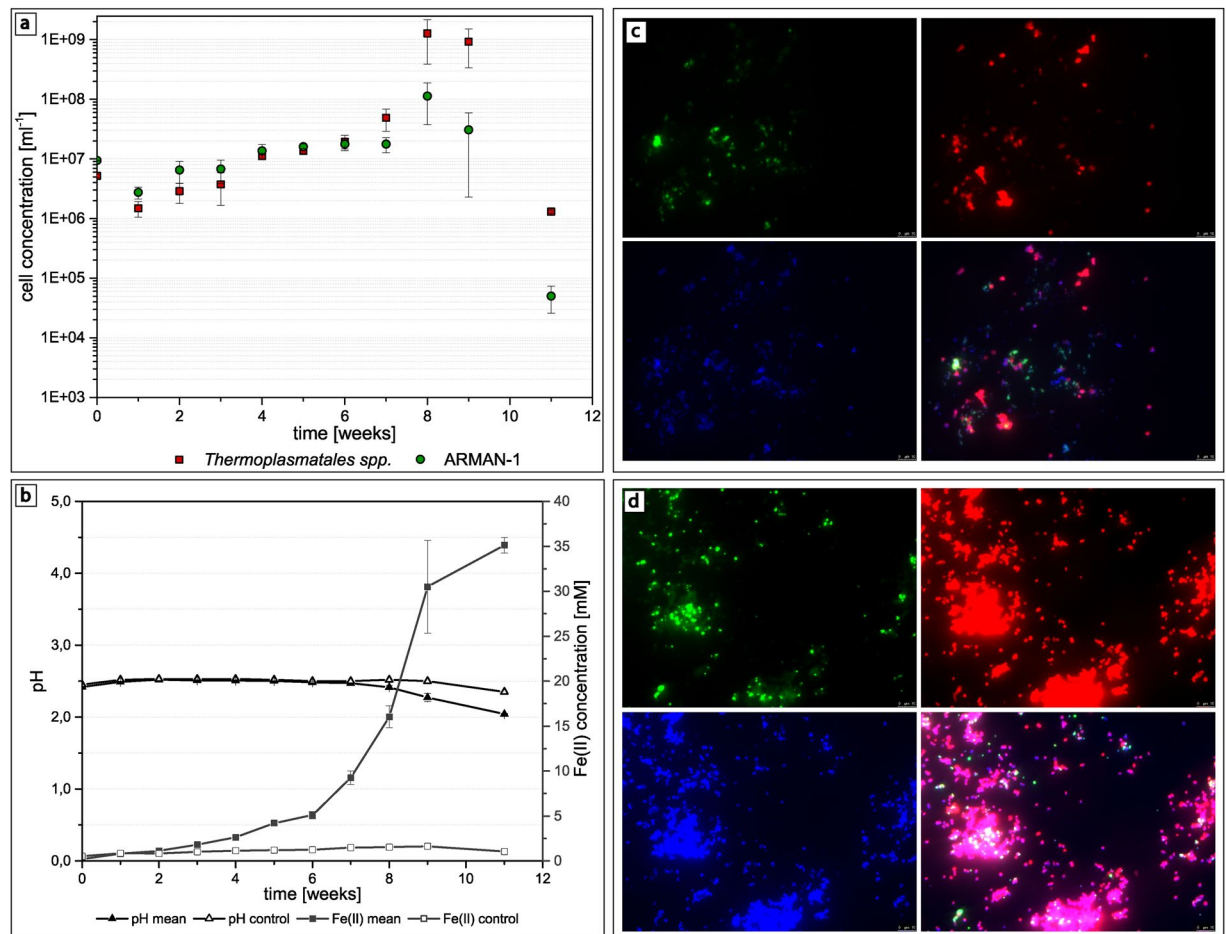


Figure 6. (a) Cell concentrations of the enrichment cultures calculated from qPCR data of A_DKE, B_DKE and C_DKE, (b) with corresponding pH values and Fe(II) concentrations over a time period of 11 weeks. Corresponding CARD-FISH pictures of enrichment cultures showing: (c) co-culture after four weeks of growth (B_DKE and C_DKE stained in red (ARCH915, Alexa 546) and A_DKE stained in green (ARM980, Alexa 488)) and (d) after eight weeks of growth (again B_DKE and C_DKE stained in red (ARCH915, Alexa 546) and A_DKE stained in green (ARM980, Alexa 488)).

Conclusion

We established a highly enriched consortium consisting of two acidophilic *Thermoplasmatales* species, an ARMAN, and a fungus. Of note, this is the only stable enrichment culture described so far containing ARMAN organisms. During the course of writing this manuscript, it was possible to obtain a culture that is composed only of A_DKE, B_DKE and the fungus (data not shown). Hence, we cannot say whether a specific archaeon is necessary to sustain growth of the ARMAN, but at least the interaction with B_DKE seems to be sufficient.

The cultivated ARMAN-1 has a complete or nearly complete TCA cycle and lacks nearly all enzymes necessary for glycolysis/glyconeogenesis and the pentose phosphate pathway. Moreover, we could not find evidence for gluconeogenesis and the pentose phosphate pathway, suggesting a dependency on synthesis of hexose and pentose sugars by other community members. This dependency seems to be corroborated by the identification of ARMAN cells within biofilm flocks that are likely built primarily by B_DKE. The colocalization of the cells might simplify access to suitable carbohydrates for the ARMAN. At least B_DKE seem to thrive using a respiratory metabolism with ferric iron as electron acceptor. Very recently, the sequence of another ARMAN-1 genome was published³⁹. It will be interesting to study differences in the genomes obtained from the US and German field sites in future studies.

We tried to exclude oxygen from the growth medium and measurements of the oxygen content of the cultures by an optode suggest an anaerobic lifestyle. Moreover, similar growth of the archaea was also observed in an anoxic glove box. The reatively high expression levels of genes corresponding to enzymes involved in the elimination of oxidative stress might be due to the relatively short exposure to oxygen at the point of RNA sampling. In future experiments, we will combine heat inactivated B_DKE/fungus extracts with filtration based selection for pure ARMAN cultures. Nevertheless, B_DKE cells are also very small and pleomorphic, and the doubling time of the organisms is rather low. Hence, although future experiments seem straight forward they will require months or years of incubation time for several necessary culture transfers.

Experimental Procedures

Culturing conditions. Enrichment cultures of *Thermoplasma* spp. and ARMAN-1 originate from acidophilic stalactite-like biofilms of the former pyrite-mine “Drei Kronen und Ehrt” in the Harz Mountains, Germany (Ziegler *et al.* ^{24,25}). Biofilms were inoculated under anoxic conditions in Hungate tubes and in a medium originally designed for the isolation of *Picrophilus* species⁴⁰. The pH of the medium was adjusted to 2.5 using 0.5 M H₂SO₄. Afterwards, the medium was autoclaved and supplemented with sterile filtered solutions of yeast extract, casein and ferric sulfate to final concentrations of 0.1% each and 20 mM, respectively, as critical additives. The growth of the bacterial species was repressed with 150 µg ml⁻¹ streptomycin, 50 µg ml⁻¹ kanamycin, 30 µg ml⁻¹ chloramphenicol and 2 µg ml⁻¹ vancomycin. The headspace was flushed with an 80% H₂/CO₂ 20% gas mixture. Cultures were inoculated with 10% of a growing co-culture and incubated at 22 °C. *Escherichia coli* cells were routinely cultured in LB medium supplemented with 40 µg ml⁻¹ kanamycin or 100 µg ml⁻¹ ampicillin, if necessary. Isolation of a fungus was conducted with a medium based on the study by Baker *et al.*³⁷. The pH of the medium was adjusted to 2 using 0.5 M H₂SO₄ and it was supplemented with SL10 trace elements (DSMZ medium 320). The media plates were prepared with the addition of 2% (w/v) agar.

CARD-FISH. Samples were fixed for 1 h in 4% paraformaldehyde, washed twice in phosphate-buffered saline (PBS) and stored at -20 °C in 50:50 PBS/ethanol. The fixed cells were hybridized and amplified as described previously^{25,41,42}. The following HRP-labelled 16S rDNA probes were used: ARCH915 (Archaea domain, GTG CTC CCC CGC CAA TTC CT, 20% formamide⁴²) and ARM980 (ARMAN, GCC GTC GCT TCT GGT AAT, 30% formamide¹⁹). For amplification, Alexa₅₄₆ and Alexa₄₈₈ were used and counterstaining was conducted with DAPI. Samples were viewed on a Leica DM 5500B microscope (object lens 100x: HCX PL FLUOTAR, 1.4, oil immersion; eyepiece 10x: HC PLAN s (25) M), and images were taken with a Leica DFC 360 FX camera and the corresponding Leica LAS AF Lite software.

Ferrous iron quantification. Ferric iron reduction was determined by quantification of the ferrous iron content spectrophotometrically using the ferrozine assay as described previously⁴³.

Isolation of fungal DNA and amplification. A protocol based on Cenis (1992)⁴⁴ was used to isolate DNA from the fungus. For taxonomic classification, the internal transcribed spacer (ITS) region primers ITS1 and ITS4⁴⁵ were used to amplify the DNA with the iProof™ High-Fidelity PCR Kit (Bio-Rad, Munich, Germany).

Quantification of cells using quantitative PCR. Quantitative PCR was used to quantify growth of the archaeal species in the enrichment culture. Standard curves were developed by integrating plasmids containing the target sequences of the qPCR primer sets in the genome of *E. coli*. Primer sets were developed for the 23S rRNA gene of ARMAN-1 and the 23S rRNA of the two *Thermoplasma* spp. using NCBI/Primer-BLAST⁴⁶ as described in the supplemental information. The primer sequences are listed in Supplementary Table S9.

The organisms could contain more than one copy of the 23S rRNA gene, and this would hamper quantitative analysis. Thus, the normalized per-sample coverage of all genes was compared to the 23S rRNA gene coverage. The latter was always below the overall coverage (Supplementary Table S10). Hence, the assumption was made that the 23S rRNA was represented by one copy in the genome.

DNA/RNA isolation for metagenomics/metatranscriptomics. Isolation of genomic DNA for metagenomic analysis was conducted according to Lo *et al.*⁴⁷. The total RNA isolation was conducted according to the protocol of the TRIzol Max Bacterial RNA Isolation Kit (Thermo Fisher, Waltham, USA) with 8 ml of an enrichment culture as the starting material. The remaining DNA was hydrolyzed with the DNA-free™ DNA Removal Kit (Thermo Fisher, Waltham, USA) following the manufacturer’s instructions.

Metagenomic/metatranscriptomic sequencing and analyses. Metagenomic DNA from two analogous enrichment cultures was used for Illumina-based sequencing using a 2 × 51 bp protocol. The metatranscriptomic analysis was based on an RNA isolation from 8 mL of the enrichment culture. This sample was pooled from analogous enrichment cultures with similar growth characteristics. The RNA was sequenced using the 2 × 100 bp protocol. Supplementary Table S11 shows the overall statistics of the sequencing experiments.

Data availability. All DNA and RNA sequences that were retrieved within this study are publically available through NCBI BioProject: PRJNA358824.

16S rDNA gene sequence of B_DKE and 18S rDNA/ITS gene sequence of the fungus are available through NCBI GenBank accession numbers KY825129 and KY848528.

References

- Steering G for the Workshop on Size Limits of Very Small Microorganisms, National Research Council. in *Size Limits of Very Small Microorganisms: Proceedings of a Workshop 5–7* (National Academies Press, 1999).
- Torrella, F. & Morita, R. Y. Microcultural study of bacterial size changes and microcolony and ultramicrocolony formation by heterotrophic bacteria in seawater. *Appl. Environ. Microbiol.* **41**, 518–527 (1981).
- Bae, H. C., Cota-Robles, E. H. & Casida, L. E. Microflora of soil as viewed by transmission electron microscopy. *Appl. Microbiol.* **23**, 637–648 (1972).
- Folk, R. L. SEM imaging of bacteria and nanobacteria in carbonate sediments and rocks. *J. Sediment. Petrol.* **63**, 990–999 (1993).
- Kajander, E. O. & Ciftcioglu, N. Nanobacteria: an alternative mechanism for pathogenic intra- and extracellular calcification and stone formation. *Proc. Natl. Acad. Sci. USA* **95**, 8274–8279 (1998).
- Cisar, J. O. *et al.* An alternative interpretation of nanobacteria-induced biomineralization. *Proc. Natl. Acad. Sci.* **97**, 11511–11515 (2000).
- Kjelleberg, S. No Title. in *Trends in Microbial Ecology* (eds. Guerrero, R. & Pedros-Alio, C.) (Spanish Society for Microbiology, 1993).

8. Miyoshi, T., Iwatsuki, T. & Naganuma, T. Phylogenetic characterization of 16S rRNA gene clones from deep-groundwater microorganisms that pass through 0.2-micrometer-pore-size filters. *Appl. Environ. Microbiol.* **71**, 1084–1088 (2005).
9. Luef, B. *et al.* Diverse uncultivated ultra-small bacterial cells in groundwater. *Nat. Commun.* **6**, 6372 (2015).
10. Hahn, M. W. *et al.* Isolation of novel ultramicrobacteria classified as actinobacteria from five freshwater habitats in Europe and Asia. *Appl. Environ. Microbiol.* **69**, 1442–1451 (2003).
11. Suzina, N. E. *et al.* Novel ultramicrobacteria, strains NF4 and NF5, of the genus *Chryseobacterium*: Facultative epibionts of *Bacillus subtilis*. *Microbiology* **80**, 535–548 (2011).
12. Duda, V. I. *et al.* A cytological characterization of the parasitic action of ultramicrobacteria NF1 and NF3 of the genus *Kaistia* on chemoorganotrophic and phototrophic bacteria. *FEMS Microbiol. Ecol.* **69**, 180–193 (2009).
13. Rappé, M. S., Connon, S., Vergin, K. L. & Giovannoni, S. J. Cultivation of the ubiquitous SAR11 marine bacterioplankton clade. *Nature* **418**, 630–633 (2002).
14. Waters, E. *et al.* The genome of *Nanoarchaeum equitans*: insights into early archaeal evolution and derived parasitism. *Proc. Natl. Acad. Sci. USA* **100**, 12984–8 (2003).
15. Jahn, U. *et al.* *Nanoarchaeum equitans* and *Ignicoccus hospitalis*: New insights into a unique, intimate association of two archaea. *J. Bacteriol.* **190**, 1743–1750 (2008).
16. Giannone, R. J. *et al.* Life on the edge: functional genomic response of *Ignicoccus hospitalis* to the presence of *Nanoarchaeum equitans*. *ISME J.* **9**, 101–14 (2015).
17. Wurch, L. *et al.* Genomics-informed isolation and characterization of a symbiotic Nanoarchaeota system from a terrestrial geothermal environment. *Nat. Commun.* **7**, 1–10 (2016).
18. Baker, B. J. *et al.* Enigmatic, ultrasmall, uncultivated Archaea. *Proc. Natl. Acad. Sci. USA* **107**, 8806–8811 (2010).
19. Baker, B. J. *et al.* Lineages of acidophilic archaea revealed by community genomic analysis. *Science* **314**, 1933–1935 (2006).
20. Comolli, L. R., Baker, B. J., Downing, K. H., Siegerist, C. E. & Banfield, J. F. Three-dimensional analysis of the structure and ecology of a novel, ultra-small archaeon. *ISME J.* **3**, 159–167 (2009).
21. Justice, N. B. *et al.* Heterotrophic archaea contribute to carbon cycling in low-pH, suboxic biofilm communities. *Appl. Environ. Microbiol.* **78**, 8321–8330 (2012).
22. Amaral-Zettler, L. A. *et al.* Microbial community structure across the tree of life in the extreme Río Tinto. *ISME J.* **5**, 42–50 (2011).
23. Méndez-García, C. *et al.* Microbial stratification in low pH oxic and suboxic macroscopic growths along an acid mine drainage. *ISME J.* **8**, 1259–74 (2014).
24. Ziegler, S., Ackermann, S., Majzlan, J. & Gescher, J. Matrix composition and community structure analysis of a novel bacterial pyrite leaching community. *Environ. Microbiol.* **11**, 2329–2338 (2009).
25. Ziegler, S. *et al.* Oxygen-dependent niche formation of a pyrite-dependent acidophilic consortium built by archaea and bacteria. *ISME J.* **7**, 1725–1737 (2013).
26. Droege, J., Gregor, I. & McHardy, A. C. Taxator-tk: Precise taxonomic assignment of metagenomes by fast approximation of evolutionary neighborhoods. *Bioinformatics* **31**, 817–824 (2015).
27. Golyshina, O. V. *et al.* The novel extremely acidophilic, cell-wall-deficient archaeon *Cuniculiplasma divulgatum* gen. nov., sp. nov. represents a new family, *Cuniculiplasmataceae* fam. nov., of the order *Thermoplasmatales*. *Int. J. Syst. Evol. Microbiol.* **66**, 332–340 (2016).
28. Yelton, A. P. *et al.* Comparative genomics in acid mine drainage biofilm communities reveals metabolic and structural differentiation of co-occurring archaea. *BMC Genomics* **14**, 485 (2013).
29. Schäfer, G., Engelhard, M. & Müller, V. Bioenergetics of the Archaea. *Microbiol. Mol. Biol. Rev.* **63**, 570–620 (1999).
30. Bräsen, C., Esser, D., Rauch, B. & Siebers, B. Carbohydrate metabolism in Archaea: current insights into unusual enzymes and pathways and their regulation. *Microbiol. Mol. Biol. Rev.* **78**, 89–175 (2014).
31. Budgen, N. & Danson, M. J. Metabolism of glucose via a modified Entner-Doudoroff pathway in the thermoacidophilic archaeobacterium *Thermoplasma acidophilum*. *FEBS Lett.* **196**, 207–210 (1986).
32. Reher, M., Fuhrer, T., Bott, M. & Schönheit, P. The nonphosphorylative entner-doudoroff pathway in the thermoacidophilic euryarchaeon *Picrophilus torridus* involves a novel 2-Keto-3-deoxygluconate-specific aldolase. *J. Bacteriol.* **192**, 964–974 (2010).
33. Golyshina, O. V. *et al.* Biology of archaea from a novel family *Cuniculiplasmataceae* (Thermoplasmata) ubiquitous in hyperacidic environments. *Sci. Rep.* **6**, 39034 (2016).
34. Ruepp, A. *et al.* The genome sequence of the thermoacidophilic scavenger *Thermoplasma acidophilum*. *Nature* **407**, 508–513 (2000).
35. Fütterer, O. *et al.* Genome sequence of *Picrophilus torridus* and its implications for life around pH 0. *Proc. Natl. Acad. Sci. USA* **101**, 9091–9096 (2004).
36. Say, R. F. & Fuchs, G. Fructose 1,6-bisphosphate aldolase/phosphatase may be an ancestral gluconeogenic enzyme. *Nature* **464**, 1077–1081 (2010).
37. Baker, B. J., Lutz, M. A., Dawson, S. C., Bond, P. L. & Banfield, J. F. Metabolically active eukaryotic communities in extremely acidic mine drainage. *Appl. Environ. Microbiol.* **70**, 6264–6271 (2004).
38. Hujšlová, M., Kubátová, A., Kostov, M., Blanchette, R. A. & Beer, Z. W. De. *Three new genera of fungi from extremely acidic soils*. *Mycol. Prog.* **13**, 819–831 (2014).
39. Burstein, D. *et al.* New CRISPR-Cas systems from uncultivated microbes. *Nat. Lett.* **542**, 237–241 (2017).
40. Huber, H. & Stetter, K. O. in *The Prokaryotes: An evolving electronic resource for the microbiological community* (eds. Dworkin, M., Falkow, S., Rosenberg, E., Schleifer, K.-H. & Stackebrandt, E.) (Springer, 2001).
41. Pernthaler, A., Pernthaler, J. & Amann, R. Sensitive multi-color fluorescence *in situ* hybridization for the identification of environmental microorganisms. *Mol. Microb. Ecol. Man.* **3**, 711–726 (2004).
42. Stahl, D. A. & Amann, R. in *Nucleic acid techniques in bacterial systematics* (eds. Stackebrandt, E. & Goodfellow, M.) 205–242 (Wiley, 1991).
43. Stookey, L. L. Ferrozine - a new spectrophotometric reagent for iron. *Anal. Chem.* **42**, 779–781 (1970).
44. Cenis, J. L. Rapid extraction of fungal DNA for PCR amplification. *Nucleic Acids Res.* **20**, 2380 (1992).
45. White, T. J., Bruns, T., Lee, S. & Taylor, J. in *PCR protocols: a guide to methods and applications*. (eds. Innis, M. A., Gelfand, D. H., Sninsky, J. & White, T. J.) 315–322 (Academic Press Inc, 1990).
46. Ye, J. *et al.* Primer-BLAST: A tool to design target-specific primers for polymerase chain reaction. *BMC Bioinformatics* **13**, 134 (2012).
47. Lo, I. *et al.* Strain-resolved community proteomics reveals recombining genomes of acidophilic bacteria. *Nature* **446**, 537–541 (2007).

Acknowledgements

We gratefully thank Dr. Sibylle Bartsch and Dr. Katharina Geiger for fruitful discussions and are grateful for funding by the DFG.

Author Contributions

S.K. – did culturing experiments, wrote main manuscript file, prepared figure 1, figure 5 and figure 6. A.B. – did bioinformatic analysis of metagenomic and metatranscriptomic data. P.C.M. – prepared figure 2, figure 3 and figure 4. A.C.Mc.H. – supervised the bioinformatic part. J.G. – supervised the work. All authors reviewed the manuscript.

Additional Information

Supplementary information accompanies this paper at doi:[10.1038/s41598-017-03315-6](https://doi.org/10.1038/s41598-017-03315-6)

Competing Interests: The authors declare that they have no competing interests.

Publisher's note: Springer Nature remains neutral with regard to jurisdictional claims in published maps and institutional affiliations.



Open Access This article is licensed under a Creative Commons Attribution 4.0 International License, which permits use, sharing, adaptation, distribution and reproduction in any medium or format, as long as you give appropriate credit to the original author(s) and the source, provide a link to the Creative Commons license, and indicate if changes were made. The images or other third party material in this article are included in the article's Creative Commons license, unless indicated otherwise in a credit line to the material. If material is not included in the article's Creative Commons license and your intended use is not permitted by statutory regulation or exceeds the permitted use, you will need to obtain permission directly from the copyright holder. To view a copy of this license, visit <http://creativecommons.org/licenses/by/4.0/>.

© The Author(s) 2017